Electronic Structure of Discrete Pseudotetrahedral Oxovanadium Centers Dispersed in a Silica Xerogel Matrix: Implications for Catalysis and Photocatalysis

ARTICLE *in* JOURNAL OF THE AMERICAN CHEMICAL SOCIETY · MARCH 1995

Impact Factor: 12.11 · DOI: 10.1021/ja00114a026

5 AUTHORS, INCLUDING:

A. E. Stiegman
Florida State University
109 PUBLICATIONS **2,220** CITATIONS

Electronic Structure of Discrete Pseudotetrahedral Oxovanadium Centers Dispersed in a Silica Xerogel Matrix: Implications for Catalysis and Photocatalysis

Kim Tran,[†] Mark A. Hanning-Lee,[‡] Abhijit Biswas,[‡] A. E. Stiegman,*[,‡,§] and Gary W. Scott*[,†]

Contribution from the Jet Propulsion Laboratory, California Institute of Technology, 4800 Oak Grove Drive, Pasadena, California, 91109, and the Department of Chemistry, University of California, Riverside, Riverside, California, 92521

Received August 24, 1994[⊗]

Abstract: The electronic structure of psuedotetrahedral oxovanadium groups ($-O_3V{=}O$) dispersed in a silica xerogel matrix, is determined on the basis of a spectroscopic investigation. From this investigation it was found that the highest occupied molecular orbital of this species is a nonbonding a_2 symmetry orbital localized on the basal plane ligands. The first excited state is assigned to an E symmetry triplet resulting from a one-electron promotion from this a_2 nonbonding orbital to an e symmetry antibonding orbital of the terminal V=O group. On the basis of this orbital description, the long-lived, vibronically structured emission at 549 nm is assigned to a $^3E \rightarrow {}^1A_1$ transition from the e antibonding orbital back down to the a_2 nonbonding orbital $[(a_2)^1(e^*)^1] \rightarrow [(a_2)^2(e^*)]$. The vibronic progression in the emission band at 977 ± 10 cm^{-1}, previously assigned to the terminal V=O stretch, is reassigned to a V−O stretch involving the basal plane oxygens, consistent with the orbital assignment. Contrary to previous descriptions, excitations involving $\pi \rightarrow \pi^*$ type transitions localized on the terminal V=O group lie at higher energy. The first well-resolved singlet band at 290 nm is of A_1 symmetry and has a resolved vibronic progression which corresponds to the terminal V=O stretch. This band is assigned to a $^1A_1 \rightarrow {}^1A_1$ transition involving a $[(e)^4(a_2)^2(e^*)] \rightarrow [(e)^3(a_2)^2(e^*)^1]$ one-electron promotion which can qualitatively be described as a "$\pi-\pi^*$" V=O transition. The electronic structure of the pseudotetrahedral oxovanadium group established in this study differs dramatically from the conventionally accepted model which localizes the ground and first excited state on the terminal V=O group. This new description, however, is completely consistent with observed photochemical processes and, unlike the previous model, provides a coherent explanation of how factors such as the nature of the substrate directly affect the oxovanadium center.

Vanadium oxide dispersed on metal and semimetal oxide supports catalyze a number of important reactions. Catalysts of this type have been used for the selective catalytic oxidation (SCO) of a number of substrates, including aliphatic and aromatic hydrocarbons, and for the selective catalytic reduction (SCR) of nitric oxide with ammonia.[1] In addition, a number of photochemically induced transformations such as the photooxidation of CO, the photoisomerization of butene, and the photopolymerization of acetylene have also been observed.[2,3] The reactivity and selectivity of these catalyst systems is highly dependent on the substrate on which the oxovanadium is dispersed and in some cases on the specific crystallographic phase of that substrate.[4] Increasingly, studies of these catalysts have suggested that substrates with monolayer or submonolayer oxovanadium coverage form, in many cases, the most reactive catalysts. This heightened reactivity is attributed to the presence of discrete oxovanadium centers in a pseudotetrahedral coordination environment which are bound to the substrate.

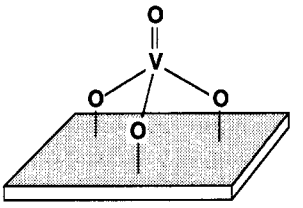

The structure of these groups which have one short terminal and three long basal plane vanadium−oxygen bonds has been characterized unambiguously by vibrational spectroscopy and solid-state NMR techniques.[5] The unique properties of the supported pseudotetrahedral oxovanadium group in the ground state have been invoked to explain thermal transformations while particular excited state properties have been proposed to explain the observed photochemistry.

To fully understand the strong synergism between this oxometal group and the various substrates to which it is bound, it is necessary to understand its electronic structure in detail. In particular, the nature of the ground and excited electronic states

[†] University of California, Riverside.

[‡] California Institute of Technology.

[§] Current address: Dept. of Chemistry, Florida State University, Tallahassee, FL 32306.

[⊗] Abstract published in *Advance ACS Abstracts,* February 1, 1995.

(1) (a) Oyama, S. T. *Res. Chem. Inter.* **1991**, *15*, 165. (b) Bond, G. C.; Tahir, S. F. *Appl. Catal.* **1991**, *71*, 1.

(2) (a) Anpo, M.; Tanahashi, I.; Kubokawa *J. Phys. Chem.* **1980**, *84*, 3440. (b) Anpo, M.; Sunamoto, M.; Che, M. *J. Phys. Chem.* **1989**, *93*, 1187.

(3) Stiegman, A. E.; Eckert, H ; Plett, G.; Anderson, M.; Yavrouian, A. *Chem. Mater.* **1993**, *5*, 1592.

(4) Cristiani, C.; Forzatti, P.; Busca, G. *J. Catal.* **1989**, *116*, 586 and references therein.

(5) (a) Oyama, S. T.; Went, G. T.; Lewis, K. B.; Bell, A. T.; Somorjai, G. A. *J. Phys. Chem.* **1989**, *93*, 6786. (b) Eckert, H.; Wachs, I. E. *J. Phys. Chem.* **1989**, *93*, 6796. (c) Went, G. T.; Oyama, S. T.; Bell, A. T. *J. Phys. Chem.* **1990**, *94*, 4240. (d) Schrami-Marth, M.; Wokaun, A.; Pohl, M.; Krauss, H.-L. *J. Chem. Soc., Faraday Trans.* **1991**, *87*, 2635. (e) Deo, G.; Wachs, I. E. *J. Catal.* **1991**, *129*, 307. (f) Das, N.; Eckert, H.; Hu, H.; Wachs, I. E.; Walzer, J. F.; Feher, F. J. *J. Phys. Chem.* **1993**, *97*, 8240.

0002-7863/95/1517-2618$09.00/0

and the vibronic modes that couple them to the surface will provide a necessary foundation for understanding catalytic reactivity. To date, however, the electronic structure of these species remains largely unknown; the inherently poor transparency of most bulk catalytic materials makes them less than amenable to detailed spectroscopic studies.

Recently, a new approach to making silica-supported vanadium oxide material using sol-gel chemistry has been exploited. A mixture of vanadia and silica gels has been used by Baiker et al. to produce a catalyst for the selective reduction of nitric oxides with ammonia.[6] Similarly, the co-condensation of oxovanadium trisalkoxides with tetraethyl orthosilicate has been utilized by Neumann et al. to produce catalysts for the oxidation of alkenes with hydrogen peroxide.[6] Using the same general approach but with lower concentrations of oxovanadium alkoxide, we have produced homogeneous transparent glasses containing the discrete pseudotetrahedral oxovanadium group.[3] The excellent transparency of these glasses permitted us to accomplish a detailed spectroscopic investigation of the oxovanadium functionality in a catalytically relevant environment. The results of this investigation, which we report herein, provide significant insight into the structure of this functional group and, more importantly, into the relationship between its electronic structure and its catalytic and photocatalytic activities.

Experimental Section

Oxovanadium-containing silica xerogel optical flats were synthesized as reported previously.[3] All optical flats were aged for approximately 6 months, dried for 1 week at 125 °C, and stabilized for 5 days at 500 °C. Samples used for absorption and emission spectroscopy contained 0.005 mol % vanadium, which corresponds to a 0.015 wt % loading of V_2O_5 in SiO_2. For the final volume of the stabilized optical flats this corresponded to a vanadium concentration of approximately 2.5×10^{-4} M. Brunauer–Emmett–Teller analysis of the 0.005% spectroscopic samples yielded pore volumes and surface areas of 0.38 mL/g and 412 m^2/g, respectively.

All samples were dehydrated at 200 °C for at least 2 h under a vacuum prior to each experiment. Samples were stored under vacuum and transferred under dry nitrogen to a purged spectrometer or to the sample holder of a closed cycle helium refrigerator (Air Products, Displex 202E). This refrigerator system, in conjunction with a temperature indicator and controller (Air Products, Model 3700), allowed temperature variations in the range 13–297 K. Samples used for Raman spectroscopy contained 0.5 mol % vanadium but were otherwise identical to the samples used for absorption and emission spectroscopy. Prior to the Raman experiment, the samples were dehydrated at 250 °C on a diffusion-pumped vacuum line for 18 h, at which point they had achieved a vacuum of 2×10^{-5} Torr. The quartz fluorimeter cell in which the sample was placed was then sealed off, and the experiments were conducted in situ—the sample was at no time re-exposed to the ambient atmosphere prior to the measurements.

Room temperature absorption spectra were collected on a Perkin-Elmer Lambda 9 spectrophotometer under a dry nitrogen purge. Low-temperature absorption and emission spectra were recorded with a spectrofluorimeter (Spex Fluorolog 2, Model F212). This instrument is equipped with double grating emission and excitation monochromators, a high-pressure xenon lamp (450 W) for excitation, a quantum counter (Rhodamine B as scintillator) to monitor the excitation beam intensity, and a cooled photomultiplier tube (Hamamatsu R928-P) used in photon counting mode to monitor the emission intensity.

The transmittance spectra of the oxovanadium and undoped silica flats at 14 K were obtained by simultaneously scanning both the emission and excitation monochromators of the spectrofluorimeter. Slits of 0.9 nm were set for both monochromators except in the spectral region below 275 nm where the output of the xenon lamp is relatively low and slits of 3.6 and 1.8 nm were used for the excitation and emission monochromators, respectively. The transmittance intensities collected were quantum counter ratioed to correct for the output fluctuation of the light source. The relative absorbance of the oxovanadium–silica flat at each wavelength was taken as the logarithm of the ratio of the corrected intensities transmitted through undoped and vanadia-containing silica samples at the corresponding wavelength.

Emission spectra of the oxovanadium–silica flats at 14 K were recorded with 0.9 nm slits for both monochromators of the spectrofluorimeter. Schott KV nonfluorescing filters were used to eliminate the interference of scattered excitation light. Emission intensities were quantum counter ratioed and corrected for wavelength variation of detector efficiency. In addition to the corrections described above, the emission spectrum used for the Franck–Condon analysis, which was collected at 77 K using 325 nm excitation and 1.25 and 0.5 nm emission and excitation slits, respectively, was corrected for elastic and Raman scattered light using an undoped silica flat. This correction gave better convergence to base line at the low-energy tail of the emission, which improved the accuracy of the Franck–Condon analysis.

To measure the polarization anisotropy, the steady-state excitation polarization spectra at 14 K were obtained with the spectrofluorimeter using Glan–Taylor ultraviolet and Glan–Thompson prism polarizers (Karl Lambrecht) as excitation and emission polarizers, respectively. The L-format method was utilized, and the excitation anisotropy at each wavelength was determined by

$$r = \frac{I_{VV} - GI_{VH}}{I_{VV} + 2GI_{VH}}$$

in which $G = I_{HV}/I_{HH}$. In this formula r is the anisotropy and I is the emission intensity.[7] The subscripts denote the relative orientation of the excitation and emission polarizers, respectively. For example, I_{VH} is the emission intensity corresponding to vertically-polarized excitation while detecting the horizontally-polarized emission. A polarization scrambler was inserted between the emission polarizer and the detector to ensure $G \approx 1$. Scattered light from a dilute aqueous solution to glycogen (Sigma, oyster type II) was used to align the polarizer axes relative to each other. Emission intensities were collected at 90° with respect to excitation. Polarized emission–excitation spectra were recorded by monitoring the polarized emission intensities at 625 nm while varying the excitation wavelength.

The Raman measurements were performed by interrogating vacuum-sealed oxovanadium–silica optical flats with a focused linearly polarized argon laser beam. The focused spot size incident on the sample was ~80–100 μm and the power varied from ~0.6 to 1.6 W. Inelastically scattered light from the sample following the laser incidence was collected at 90° and focused onto the entrance slit of a double monochromator without any polarization discrimination. A cooled (233 K) photomultiplier tube (PMT) detector mounted at the exit slit of the monochromator was connected to photon-counting electronics. Signal averaging of 20–40 s per point was used and the uncertainty in the Raman shift is ± 2 cm^{-1} as determined by considerations based on calibration to known wavelength lines as well as the step size used while scanning the grating of the monochromator. The Raman nature of the spectra was confirmed by obtaining identical spectral profiles over the region of interest when using both the 514.5 and 488.0 nm laser lines. The Raman band at 977 cm^{-1} was additionally verified using the 476.5 and 457 nm laser lines.

The Franck–Condon analysis was carried out using a spectral simulation program, the algorithm of which was published previously.[8] In this simulation the ground and excited electronic states are both treated as harmonic oscillators with a frequency ν. The potential curves are defined by a normal coordinate q with the two potential curves displaced relative to each other by an amount δq (the normal coordinate change). The emission intensity of the transition from the vibrationless excited state to a vibrational level n in the ground state is given by

(6) (a) Baiker, A.; Dollenmeier, P.; Glinski, M.; Reller, A.; Sharma, V. K. *J. Catal.* **1988**, *111*, 273. (b) Neumann, R.; Chava, M.; Levin, M. *J. Chem. Soc., Chem. Commun.* **1993**, 1685.

(7) Lakowicz, J. R. *Principles of Fluorescence Spectroscopy*; Plenum: New York, 1983; p 23.

(8) Miskowski, V. M.; Albin, M.; Hopkins, M. D.; Brinza, D. E.; Gray, H. B. *Comput. Chem.* **1988**, *12*, 171.

$$I_n = \text{constant} \cdot E_n^4 R_n^2$$

where E_n is the transition energy, R_n is the vibrational part of the transition dipole moment, and the constant term includes the electronic part of the transition moment; $R_n^2 = R_0^2 C_n^2$, with C_n^2 following a Poisson distribution:

$$C_n^2 = \frac{1}{n!}\left(\frac{\Delta^2}{2}\right)^n$$

$$\Delta = 2\pi\delta q\sqrt{\frac{\mu c\nu}{h}}$$

where Δ is a dimensionless displacement and μ is the reduced mass of the oscillator.[9] Simulations of experimental data can only estimate the values of Δ. The sign of δq cannot be determined as it appears only within Δ which occurs only as a squared term (Δ^2). The magnitude, however, can be determined but only if the reduced mass of the vibrating chromophore is known or can be estimated.

Franck–Condon analysis was carried out by measuring the positions of the best resolved vibronic peaks and, when possible, directly determining the position of the vibronic origin (E_{0-0} energy) from the spectra. The tabulated frequencies were analyzed to determine the number of active modes and their estimated frequency. Using these data an initial simulation was carried out from which small changes in the frequency and origin can be made in order to optimize agreement with the actual spectrum. The normal coordinate change, which is estimated initially, is then adjusted so that the relative peak intensities of the vibronic modes agree with the data. It should be pointed out that while the three parameters of the frequency, origin, and normal coordinate change are varied to optimize agreement with the data, they are interdependent and serve as an internal check as to the reasonableness of the fit. For example, if the origin is incorrectly determined, then the normal coordinate change required to bring the intensity distribution into agreement will be unphysical (i.e., anomalously large or small). The simulation is convoluted with a Gaussian line shape, and all transitions were summed to match the experimental spectrum (normalized by area). Residuals are calculated to estimate the quality of the simulation.

Results and Discussion

Absorption and emission spectroscopies were carried out on 0.4 × 0.4 × 1.2 cm optical flats of ≈2.5 × 10^{-4} M vanadium xerogel glass. The room temperature absorption spectrum obtained from these flats (Figure 1) shows two distinct bands occurring at 235 nm ($\epsilon = 5.2 \times 10^3$) and a broad band centered at 330 nm ($\epsilon = 5.0 \times 10^2$). In addition, the materials exhibit an intense, long-lived emission (11.2 ± 0.9 ms at 77 K) with a $\lambda_{max} = 549$ nm which is vibrationally structured at 77 K (Figure 2). This emission has been observed previously and attributed to a phosphorescence emanating from a triplet charge transfer state of the pseudotetrahedral oxovanadium chromophore.[10] The excitation spectrum collected at 77 K by monitoring the emission at 470 nm (Figure 2) replicates the general features of the room temperature absorption spectrum with peaks at 253 and 287 nm, thereby verifying that the emission is associated with the oxovanadium chromophore. Several things can be deduced from these spectra. First, the Stokes shift between the emission and the lowest energy observable absorption transition is anomalously large (10 921 cm^{-1}) for a chromophore in condensed media. In fact, there is no observable overlap between the emission and the absorption or excitation spectra that would coincide with a zero-point energy transition (Figure 2). Second, the extinction coefficients of the two observed transitions are much larger than those normally associated with spin forbidden singlet–triplet absorptions in transition metal complexes, which typically have values of $\epsilon < 100$. Finally, the pronounced vibronic structure observed in the emission spectrum is absent from either of the bands in the excitation spectrum (Figure 2). Taken together, these observations suggest that the two observed absorption transitions are to singlet states and that the emitting triplet state is subsequently reached by intersystem crossing. This would suggest that the absorption to the triplet state lies in the region between the emission and the first observed absorption band. This band is weak and unresolved at 298 and 77 K.

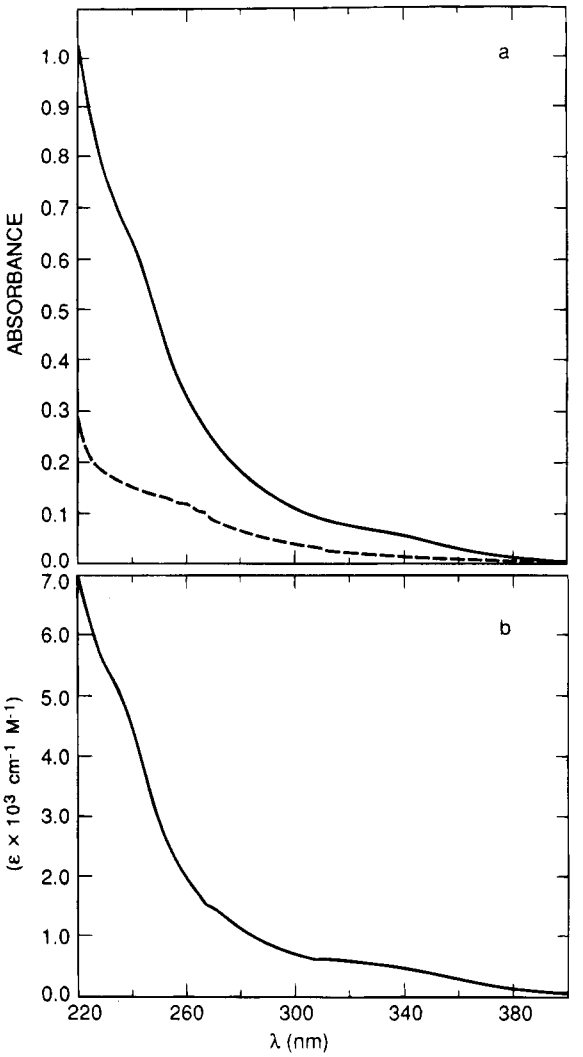

Figure 1. Room temperature absorption spectrum of (a) 0.005% oxovanadium silica sol-gel optical flat (—) and a pure silica sol-gel flat (– –) (b) and their difference spectrum.

The excitation spectrum collected at 14 K clearly shows features not apparent in the 77 K spectrum (Figure 2). The intense high-energy transition is somewhat blue-shifted while the broad low-energy band at 287 nm has been resolved into a intense peak at 290 nm and a weak but resolved shoulder at 323 nm. In addition, this newly resolved low-energy shoulder has observable intensity overlapping the emission (Figure 2 inset). The absorption spectrum of this region, also collected at 14 K (Figure 3), resolves this band unambiguously. On the basis of these data and the previous discussion, we assign this band as the direct absorption to the triplet emitting state. This assignment is further confirmed by the polarization anisotropy (Figure 4), which shows a steady increase to the single axis excitation/emission value of 0.4 at this wavelength. At this

(9) Sobolewsi, A. *Acta Phys. Polnica* **1980**, *A58*, 353.

(10) (a) Gritscov, A. M.; Shvets, V. A.; Kazansky, V. B. *Chem. Phys. Lett.* **1975**, *35*, 511. (b) Anpo, M.; Tanahashi, I.; Kubokawa, Y. *J. Phys. Chem.* **1980**, *84*, 3440. (c) Iwamoto, M.; Furukawa, H.; Matsukami, K.; Takenaka, T.; Kagawa, S. *J. Am. Chem. Soc.* **1983**, *105*, 3719.

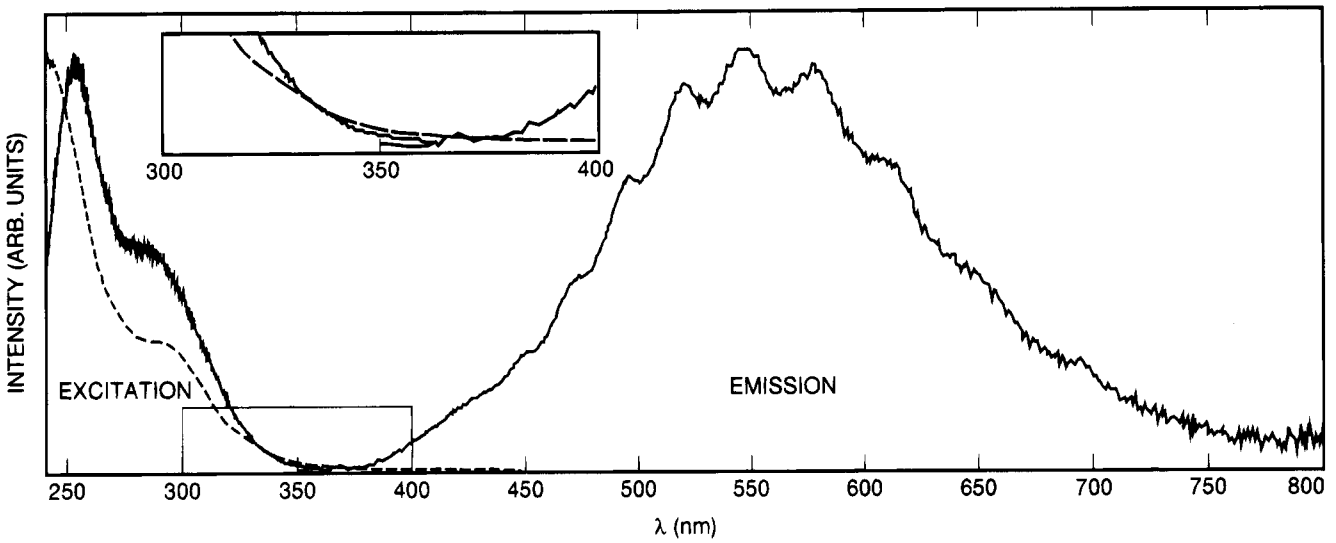

Figure 2. Emission and excitation spectrum of 0.005% oxovanadium silica sol-gel optical flat collected at 77 K (—) and 14 K (– –).

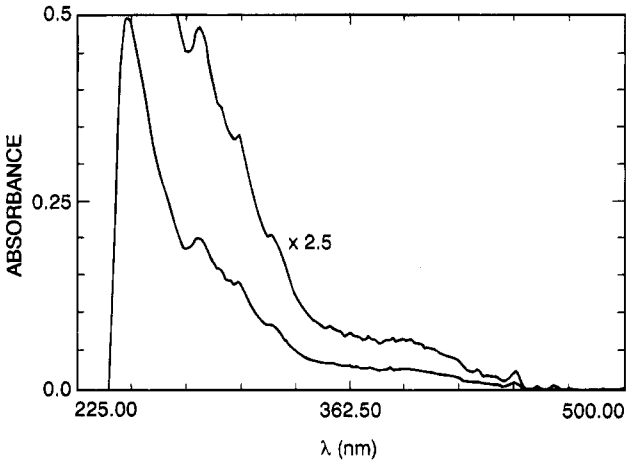

Figure 3. Absorption spectrum of 0.005% oxovanadium silica sol-gel optical flat collected at 14 K.

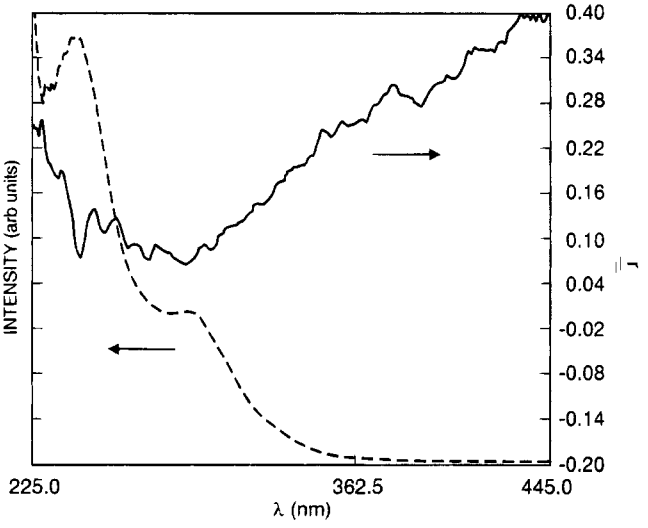

Figure 4. Polarization anisotropy (—) and excitation spectrum (– –) of a 0.005% oxovanadium silica sol-gel optical flat collected at 14 K.

point the transition ceases to overlap the first singlet band and becomes, ostensibly, a "pure" transition.

The absorption spectrum recorded at 14 K (Figure 4) does not clearly resolve the full vibronic progression of the triplet transition due to the low signal to noise. The intensity of the band, however, emerges from the base line directly under the first observable vibronic mode of the emission spectrum at 22 300 cm^{-1}, permitting its accurate assignment as the origin.

The 14 K absorption spectrum also shows a distinct vibronic progression on the 290 nm singlet state which was not previously resolved. As will be discussed, this progression is complex and differs in frequency significantly from the vibronic progression observed in the emission spectrum. In addition, the polarization anisotropy (Figure 4) drops precipitously in this region to a value of ≈0.06, which indicates that the 290 nm singlet is *not* of the same state symmetry as the triplet emitting state.

The more intense, high-energy singlet state at 240 nm shows no resolvable vibronic structure even at 14 K. The polarization anisotropy (Figure 4), however, increases going into this band and attains, ultimately, a maximum value of 0.25. It is not surprising, given the overlap between the two singlet states as well as the likely presence of other unresolved transitions in this region, that the anisotropy never acquires the single-axis/single-axis value of 0.4. We therefore believe that the symmetry of this high-energy singlet state can be assigned with some confidence as being the same as that of the first triplet state.

A group theoretical analysis of four-coordinate oxovanadium chromophores with pseudotetrahedral (C_{3v}) site symmetry is given in Figure 5. For simplicity and clarity we have assumed sp^3 hybridization of all oxygen ligands.[11] Under this hybridization scheme, one sp^3 orbital on each oxygen will be occupied in σ bonding to the metal center. For the three basal plane oxygens, an additional sp^3 orbital will be bonded to the silica substrate, leaving two to participate in π-bonding to the metal while in the case of the axial oxygen all three will be available. As there is no mixing between the axial and basal plane oxygens in C_{3v} symmetry, they can be treated separately. The three sp^3 orbitals on the axial oxygen give rise to a_1 and e symmetry terms. The a_1 symmetry-adapted orbital is simply the sum of the three sp^3 orbitals. This orbital is localized at the end of the terminal oxygen and is occupied by a lone electron pair. Though it can, in principle, mix with the p_z and d_{z^2} metal orbitals, the overlap is weak and, for all intents and purposes, it is a nonbonding orbital. The degenerate e symmetry adapted orbitals, however, mix significantly with metal d orbitals (i.e., d_{xy}, d_{xz}, d_{yz}, $d_{x^2-y^2}$) to form the bonding and antibonding pair that constitute the terminal metal–oxo π system. Including the

(11) It should be noted that the results of carrying out the group theoretical analysis on the hybridized orbital basis set is rigorously identical to those obtained using the independent s and p orbitals of the oxygen ligand.

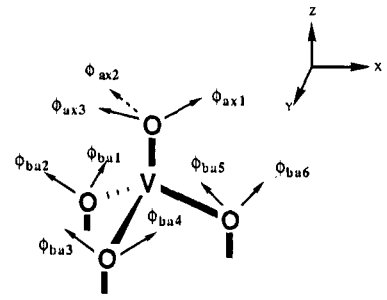

Symmetry Adapted "π" Orbitals: Axial Ligand

$$\Gamma_{\pi ax} = 3\ 0\ 1 = a_1 + e$$

$$\psi^{a_1} = [(\phi_{ax1}) + (\phi_{ax2}) + (\phi_{ax3})]$$

$$\psi^{e} = \begin{cases} [2(\phi_{ax1}) - (\phi_{ax2}) - (\phi_{ax3})] \\ [2(\phi_{ax2}) - (\phi_{ax1}) - (\phi_{ax3})] \end{cases}$$

Symmetry Adapted "π" Orbitals: Basal Plane Ligands

$$\Gamma_{\pi ba} = 6\ 0\ 0 = a_1 + a_2 + e$$

$$\psi^{a_1} = [(\phi_{ba1}) + (\phi_{ba2}) + (\phi_{ba3}) + (\phi_{ba4}) + (\phi_{ba5}) + (\phi_{ba6})]$$

$$\psi^{a_2} = [(\phi_{ba1}) + (\phi_{ba3}) + (\phi_{ba5}) - (\phi_{ba2}) - (\phi_{ba4}) - (\phi_{ba6})]$$

$$\psi^{e} = \begin{cases} [2(\phi_{ba1}) - (\phi_{ba3}) - (\phi_{ba5}) + 2(\phi_{ba2}) - (\phi_{ba4}) - (\phi_{ba6})] \\ [2(\phi_{ba1}) - (\phi_{ba3}) - (\phi_{ba5}) - 2(\phi_{ba2}) + (\phi_{ba4}) + (\phi_{ba6})] \end{cases}$$

Figure 5. Symmetry-adapted molecular orbitals for pseudotetrahedral oxovanadium center.

σ bond, this scheme yields a formal bond order of 3 for the terminal V=O group.

The basal plane oxygens give rise to all three possible symmetry terms: a_1, a_2, and e. The a_1 and e symmetry-adapted orbitals (Figure 5) mix with like-symmetry metal p and d orbitals to form three π bonds. The a_2 ligand orbital is the sum of the sp^3 orbitals on all three basal plane oxygens with nodal planes occurring at angles bisecting the ligand axes. As there are no metal orbitals spanning a_2, this ligand orbital will constitute a nonbonding molecular orbital. The bonding characteristics for this type of functional group have been analyzed in some detail using generalized valence bond (GVB) calculations. The relatively long (≈1.72 Å) basal plane metal−oxygen bonds are ionic with slight covalent character contributed through the relatively weak π bonding. We would anticipate that the formal bond order of the basal plane ligands will be considerably lower than the formal value of 2 arrived at from the simple MO diagram. The terminal V=O bond, which has a very ionic σ bond, has a large component of covalent bonding due to the π system. This covalent π bonding is enhanced by the strongly ionic character of the basal plane ligands which effectively increases the positive charge on the metal center, encouraging electron transfer from the terminal oxygen. The terminal V=O bond is therefore much stronger than the basal plane metal−oxygen bonds, and its bond order is only somewhat lower than its formal value of 3.[12] These factors play an important role in predicting the overall structure of the chromophore in both the ground and excited state.

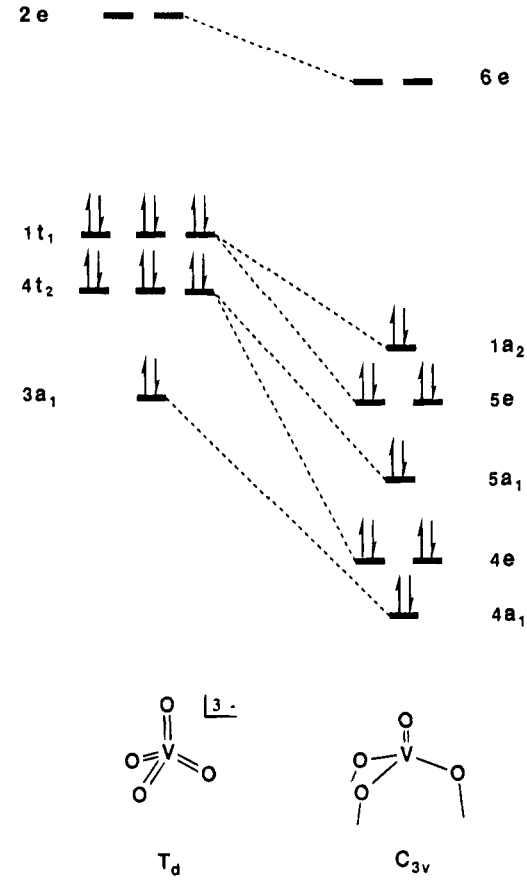

Figure 6. Molecular orbital diagram illustrating symmetry reduction of vanadate (T_d) to pseudotetrahedral oxovanadium (C_{3v}).

The highest occupied and lowest unoccupied molecular orbitals (HOMO and LUMO) for the oxovanadium species can be predicted from the well-understood electronic structure of the tetrahedral vanadate ion (VO_4^{3-}) as its symmetry is reduced from T_d to C_{3v}.[13] For the tetrahedral vanadate ion the HOMO is a nonbonding t_1 symmetry orbital while the LUMO is of e symmetry and antibonding in character. As the symmetry is reduced from T_d to C_{3v} (Figure 6), the 2e orbital is unchanged, remaining the LUMO and retaining its antibonding character (henceforth designated e*) to form the "π*" orbital of the terminal V=O bond. The t_1 HOMO, however, splits into a_2 and e symmetry orbitals. The a_2 orbital is the nonbonding orbital localized on the basal plane oxygen ligands while the e symmetry orbital, which becomes bonding in the C_{3v} point group, forms the "π" orbital of the terminal V=O group.

The specific ordering of the a_2 and e orbitals in the $-O_3V{=}O$ oxovanadium group can be predicted by analogy with other pseudotetrahedral d^0 metal complexes of the general form X_3-MY (X and Y are halogens, oxygen, or the chalcogenides) whose electronic structure and spectroscopy are well understood.[14] Compounds of this type, of which the oxovanadium center is an example, have a relative energetic ordering of the a_2 and e molecular orbitals that is usually dictated by the

(12) (a) Rappé, A. K.; Goddard, W. A., III *J. Am. Chem. Soc.* **1982**, *104*, 3287. (b) Rappé, A. K.; Goddard, W. A., III *J. Am. Chem. Soc.* **1982**, *104*, 448. (c) Allison, J. N.; Goddard, W. A. Solid State Chemistry in Catalysis. *ACS Symp. Ser.* **1985**, *279*, 23.

(13) (a) Ballhausen, C. J.; Liehr, A. D. *J. Mol. Spectrosc.* **1958**, *2*, 342. (b) Müller, A.; Diemann, E.; Ranade, A. C. *Chem. Phys. Lett.* **1969**, *3*, 467. (c) Petit, R. H.; Briat, B.; Müller, A.; Diemann, E. *Mol. Phys.* **1974**, *27*, 1373. (d) Ziegler, T.; Rauk, A.; Baerends, E. *J. Chem. Phys.* **1976**, *16*, 209.

(14) Müller, A.; Diemann, E.; Jørgensen, C. K. *Struct. Bond.* **1973**, *14*, 23.

Table 1. Frequencies (cm^{-1}) of Vibrational Modes Resolved in the 545 nm Phosphorescence of Pseudotetrahedral Oxovanadium Centers in Silica Gel

frequency	frequency change
22 181	
	1004
21 177	
	970
20 207	
	970
19 237	
	903
18 334	
	909
17 425	
mean	951 ± 39

ionization potential of the constitutive ligands. For example, due to the higher ionization potential of oxygen over sulfur, the complex S_3WO has a $(e)^4(a_2)^2(e^*)$ electron configuration with the basal plane ligands constituting the HOMO, while the O_3WS complex has just the inverse, a $(a_2)^2(e)^4(e^*)$ configuration.[15] The ionization potential of the terminal oxygen on the oxovanadium center will be higher than that of the "bridging" basal plane oxygens, making the a_2 nonbonding orbital the HOMO and yielding the $(e)^4(a_2)^2(e^*)$ occupancy scheme.[16] This orbital scheme is in agreement with those determined by tight binding extended Hückel calculations on V_2O_5 and by SCF calculation of the model compound $(HO)_3VO$.[17] The ordering of the other low-lying molecular orbitals given in Figure 6 are based on these calculations.

As mentioned, the LUMO is an e symmetry orbital which is essentially antibonding with respect to the terminal V=O bond and is composed primarily of metal (*e.g.*, $d_{x^2-y^2}$, d_{xy}, d_{xz}, d_{yz}) localized orbitals. The one-electron transition $(e)^4(a_2)^2(e^*) \rightarrow (e)^4(a_2)^1(e^*)^1$ gives an E symmetry excited state while the $(e)^4(a_2)^2(e^*) \rightarrow (e)^3(a_2)^2(e^*)^1$ gives A_1, E, and A_2 states of which transitions to the latter are symmetry forbidden. Significantly, all of these excited states will destabilize the V=O bond; however, the charge distribution over the entire oxovanadium group will differ considerably among them.

While the low-energy triplet excitation can be tentatively assigned as an $(e)^4(a_2)^2(e^*) \rightarrow (e)^4(a_2)^1(e^*)^1$ [$^1A_1 \rightarrow {}^3E$] transition on the basis of the ordering of molecular orbitals, for this assignment to be valid the well-resolved vibronic progression observed in the emission spectrum should be consistent with it. This progression, which has an average frequency of 951 ± 38 cm^{-1} in our data (Table 1), has been observed and analyzed by a number of investigators who have, without exception, assigned it to the terminal V=O stretch.[2,10,18] The emission corresponding to an $^3E \rightarrow {}^1A_1$ transition would involve the radiative decay of a vibrationally relaxed excited state into the vibrational manifold of the nonbonding a_2 orbital which is localized *entirely* on the basal plane oxygens. It is unlikely that such a transition would be coupled to a vibronic mode localized on the terminal V=O bond; instead, it would be expected to be coupled to a mode involving the basal plane ligands. In fact, for many other d^0 molecules in this point group the vibronic structure resolved in the low-energy absorption bands has been unequivocally assigned to a basal plane X−M stretch, consistent with the a_2 to e transition; there is no reason to believe that the $-O_3V{=}O$ centers will differ substantially.[19] As such, the previous assignments of the vibronic progression as a terminal V=O are inconsistent with the assignment of the electronic transition.

Scrutiny of the assignment of the vibronic mode in the emission as a terminal V=O stretch, however, clearly reveals a number of inconsistencies. The emission spectrum of our particular material shows a well-resolved vibronic progression of which the best resolved of these (0−1 through 0−6) were measured (Table 1) and found to have an average vibrational frequency of 951 ± 39 cm^{-1}. This agrees quite closely with data reported for other silica-supported oxovanadium groups. The most obvious problem with the assignment of this progression as a terminal V=O stretch is its low frequency relative to the frequency of the V=O stretch at ≈1035 cm^{-1} established by Raman spectroscopy.[4] As the emission process samples the ground state vibrational manifold, the vibronic progressions observed should be relatively close to the frequency measured by vibrational spectroscopy. In addition, the normal coordinate changes determined from previous Franck−Condon analyses of the emission spectrum are anomalously large (0.12−0.14 Å) for a distortion localized on one bond, as they imply an excited state V=O length that is as long or longer than that of the bridging basal oxygens. Given the large differences in bond order and character between the terminal and basal plane ligands which were discussed previously, this seems unlikely. For these reasons, therefore, we believe that the previous assignment of this mode as a terminal V=O stretch is questionable and that an analysis of the vibrational spectra of these materials, particularly in the ~950 cm^{-1} region of the spectrum, in conjunction with a Franck−Condon analysis of the emission spectra is required to unambiguously establish its assignment.

The infrared spectrum of these materials, which has been reported previously, shows a relatively intense band at 935 cm^{-1}, appearing as a shoulder on the intense SiO_2 stretch, that is associated with the oxovanadium group.[3] In our initial report, however, this band was incorrectly assigned to the terminal V=O stretch. The Raman spectrum (Figure 7a) of a 0.5 mol % sample, excited at 514.9 nm, shows an intense peak in this region at 977 cm^{-1} in addition to the well-established terminal V=O stretch at 1035 cm^{-1}.[4] In addition, a previously unassigned high-frequency band at 1080 cm^{-1} is also observed. The Raman spectrum of an identically prepared pure silica optical flat (Figure 7b) is relatively featureless in this region with only a broad weak band at 1025 cm^{-1} contributing slightly to the spectrum.[20] Notably, the vibrational band at 977 cm^{-1}, which has not been previously assigned, corresponds much more closely to the vibronic mode observed in the emission spectrum than does the 1035 cm^{-1} terminal V=O stretch. As will be discussed subsequently, there is ample precedence in the previously published vibrational spectra of related materials to assign this band to a basal plane V−O stretch.

The vibrational spectra of C_{3v} metal centers of the general form $X_3V{=}O$ have been completely assigned. These species have three A_1 symmetry vibrational modes, of which the highest frequency transition has been assigned unambiguously for small molecules, clusters, and oxovanadium-dispersed bulk materials as the terminal V=O stretch. In small molecules the two lower

(15) Müller, A.; Diemann, E.; Neumann, F.; Menge, R. *Chem. Phys. Lett.* **1972**, *16*, 521.

(16) The "O" ligand has a gas phase ionization potential of 13.62 eV—higher than all other ligands except "F". When oxygen ligates in a "bridging" mode (M−OR), as it does in the basal plane of the silica bound oxovanadium group, the ionization potential decreases. While ionization potentials for species of the form RO_3SiO, which would simulate the basal ligands, have not been reported, it is reasonable to assume that such a species would fall between the values for CH_3O and FO which are 8.6 and 12.77 eV, respectively (Lias, S. *J. Phys. Chem. Ref. Data* **1988**, *17*, suppl. 1).

(17) (a) Seong, S.; Yee, K.-A.; Albright, T. A. *J. Am. Chem. Soc.* **1993**, *115*, 1981−7. (b) Kobayashi, H.; Yamaguchi, M.; Tanaka, T.; Yoshida, S. *J. Chem. Soc., Faraday Trans. 1* **1985**, *81*, 1513−25.

(18) (a) Anpo, M.; Sunamoto, M.; Fuji, T.; Patterson, H.; Che, M. *Res. Chem. Inter.* **1989**, *11*, 245. (b) Patterson, H.; Cheng, J.; Despres, S.; Sunamoto, M.; Anpo, M. *J. Phys. Chem.* **1991**, *95*, 8813. (c) Hazenkamp, M. F.; Blasse, G. *J. Phys. Chem.* **1992**, *96*, 3442.

(19) (a) Jeans, D. B.; Penfield, J. D.; Day, P. *J. Chem. Soc., Dalton Trans.* **1974**, 1777. (b) Müller, A., Ahlborn, E. *Spectrochim. Acta* **1975**, *31A*, 75. (c) Brisdon, A. K.; Holloway, J. H.; Hope, E. G.; Townson, P. J.; Levason, W.; Ogden, J. S. *J. Chem. Soc., Dalton Trans.* **1991**, 3127.

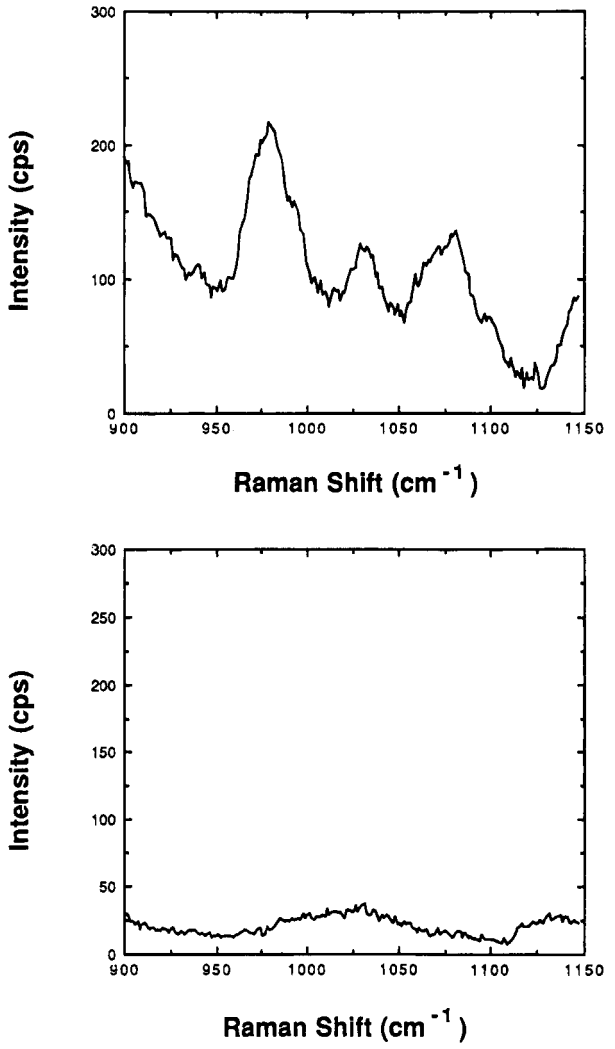

Figure 7. Raman spectrum of 0.5% oxovanadium silica sol-gel optical flat (a, top) and pure silica optical flat (b, bottom).

frequency modes have been assigned as the A_1 basal plane ligand (X−V) stretch and bend, respectively. For example, in $F_3V{=}O$ the terminal V=O stretch occurs at 1058 cm^{-1} while the basal plane F−V stretch and bend occur at 721 and 258 cm^{-1}, respectively.[21] For more extended solid systems, however, the vibrations involving the basal ligands occur at higher frequencies. The cluster $V_{10}O_{28}^{6-}$ has bands at 990 and 960 cm^{-1} which correspond to stretching modes of the terminal and the terminal plus bridging oxygens.[4c] For V_2O_5 the V−O stretch for the basal plane ligands occurs at 815 and 701 cm^{-1} (there are two distinct basal plane V−O bonds in V_2O_5, each with an associated vibrational frequency).[22] For Ti^{4+} dispersed in silica, the vibrational band occurring at 960 cm^{-1} has been discussed in some detail and has been assigned with some certainty to a stretching mode involving the $Ti{-}OSiO_3$ group.[23] On the basis of this data, we believe that it is entirely reasonable to assign the 977 cm^{-1} band in the Raman spectrum to a basal plane V−O stretch.

An excellent Franck−Condon fit of the emission spectrum is obtained (Figure 8a) using the spectroscopically determined origin at 22 300 cm^{-1}, a 977 cm^{-1} vibronic progression obtained from the Raman spectrum, and a normal coordinate change of 0.081 Å. Significantly, this fit was obtained using a reduced mass (μ) of 62, corresponding to the V=O group (taken as a unit) stretching from the basal plane. As suggested by the residuals (Figure 8b) this is an extremely good fit with the deviations due to anharmonicity not becoming evident until the (0−7) mode of the progression. By varying the frequency used in the fit over a small range, an error of ±10 cm^{-1} can be estimated. It is important to note that attempts to rationalize the vibronic progression in terms of a terminal V=O stretch always resulted in a much poorer fit and were accompanied by anomalously large normal coordinate changes. For example, consistent with previous Franck−Condon analyses, it is possible to achieve a reasonable, though substantially poorer, fit of the emission spectrum at the same frequency (977 cm^{-1}) if a terminal V=O stretch (μ = 16) is assumed; however, an unreasonable normal coordinate change of 0.18 Å is required to accomplish this. Similarly, it was impossible to simulate the spectrum in any way using a high-frequency progression (>1000 cm^{-1}) which would be more consistent with the terminal V=O stretch.

Clearly, the data presented above strongly support the assignment of the vibrational band at 977 cm^{-1} in the Raman spectrum as the active mode of the vibronic progression in the emission spectrum. In turn, we believe this band can be assigned with some confidence to the A_1 symmetry metal−oxygen stretch of the basal plane ligands. Taken together, these assignments are consistent with a low-energy excited state resulting from a basal plane ligand-to-metal-charge-transfer transition $[(a_2)^2(e^*) \rightarrow (a_2)^1(e^*)^1; [^1A_1 \rightarrow {}^3E]]$. It should be noted that an extremely self-consistent picture of the ground and first excited state electronic structure for these species emerges from these assignments.

With the assignment of the lowest energy triplet transition, the two singlet states at 290 and 240 nm can be assigned in a relatively straightforward manner. As mentioned previously, the polarization anisotropy (Figure 4) attains a value of ≈0.06 as it approaches the 290 nm peak of the first singlet state, suggesting that it is of a different symmetry than the low-energy triplet. This state, therefore, cannot be the singlet associated with the $(a_2)^2(e^*) \rightarrow (a_2)^1(e^*)^1$ $[^1A_1 \rightarrow {}^1E]$ transition and is therefore assigned to the $^1A_1$ state of the $(e)^4(a_2)^2(e^*) \rightarrow (e)^3(a_2)^2(e^*)^1$ ("$\pi \rightarrow \pi^*$" V=O) one electron transition.[24]

As was also noted previouly, the polarization anisotropy increases rapidly as it approaches the high-energy singlet state at λ_{max} = 240 nm, indicating that it is also an E symmetry state.

(20) It should be noted that the Raman spectra of these materials differ somewhat from those published previously for oxovanadium deposited on a silica surface. As these data are collected from thick optically transparent flats, it is possible to obtain spectra whose signal and resolution are orders of magnitude greater than those obtained from surface scattering from equally dilute samples. In addition, we are collecting spectral data primarily from the center of the silica matrix which can be expected to differ from species concentrated on the surface. For example, the relatively strong 975 cm^{-1} band on the surface of pure silica gel due to the Si−O stretch is extremely weak. Furthermore, the band observed at 1090 cm^{-1} is observed in surface-dispersed oxovanadium only in hydrated materials, leading to its assignment as the V=O stretch of a hydrated vanadium center. While our materials are not hydrated, it is likely that this band is due to similar interactions of the V=O group with the SiOH groups of the matrix. It should be noted that crushing the optical flat and collecting the surface Raman spectrum replicates the previously reported spectra.

(21) Selig, H.; Claassen, H. H. *J. Chem. Phys.* **1966**, *44*, 1404.

(22) Abello, L.; Husson, E.; Repelin, Y.; Lucazeau, G. *Spectrochim. Acta* **1983**, *39A*, 641.

(23) (a) Zecchina, A.; Spoto, G.; Bordiga, S.; Ferrero, A.; Petrini, G.; Leofanti, G.; Padovan, M. In *Zeolite Chemistry and Catalysis*; Jacobs, P. A. et al., Eds.; Elsevier: Amsterdam, 1991; p 251. (b) Boccuti, M. R.; Rao, K. M.; Zecchina, A.; Leofanti, G.; Petrini, G. In *Structure and Reactivity of Surfaces*; Morterra, C., Zecchina, A., Costa, G., Eds.; Elsevier: Amsterdam, 1989; p 133.

(24) This assignment is based on the fact that in C_{3v} symmetry only transitions to A_1 and E states are allowed. For the singlet state to be of different symmetry than the low-lying triplet, it can only be an A_1 state which can only come about from the $(e)^3(a_2)^2(e)^1$ configuration. While this is the most reasonable assignment, we of course cannot rule out an A_2 state which steals intensity from an A_1 state.

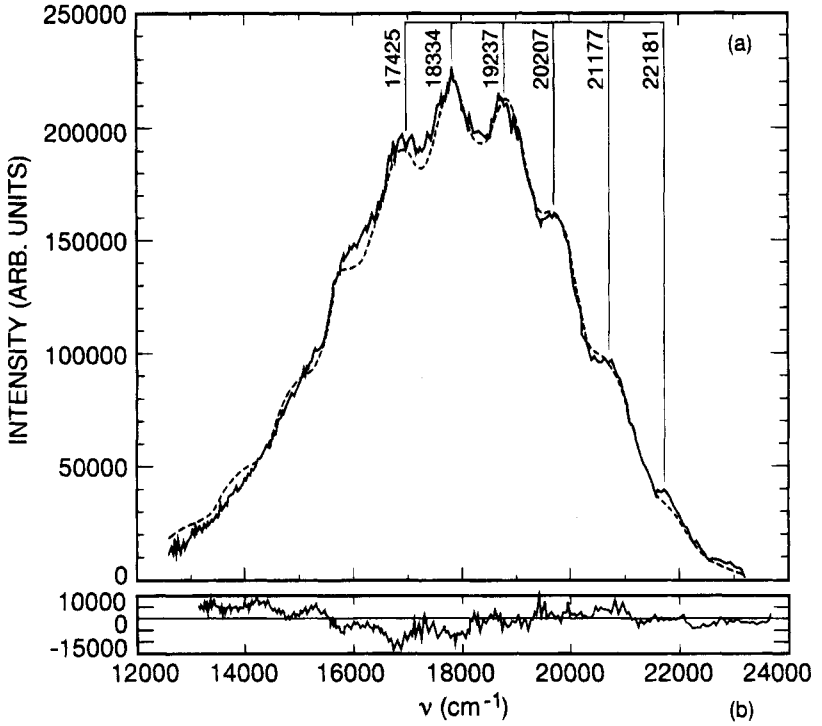

Figure 8. Franck–Condon fit (– –) of emission spectrum (—) of 0.005% oxovanadium silica sol-gel optical flat collected at 77 K (a) and the difference between the data and the simulated fit (residuals) (b).

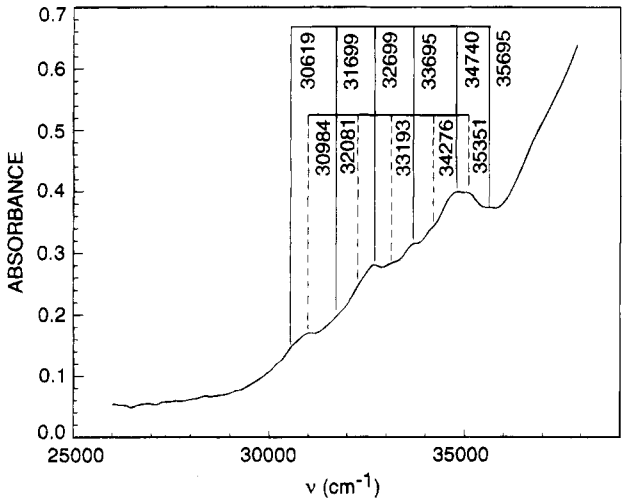

Figure 9. Absorption spectrum of 290 nm singlet at 14 K showing resolved vibronic progressions in 1015 and 1090 cm^{-1} modes.

We can, with some confidence, assign this transition to the ^1E state arising from the $(e)^4(a_2)^2(e^*) \rightarrow (e)^3(a_2)^2(e^*)^1$ one-electron transition [$^1A_1 \rightarrow {}^1E$]. The alternative to this assignment would be the ^1E state accompanying the lowest excited triplet state; such an assignment, however, would give an unlikely singlet–triplet splitting (>10 000 cm^{-1}).

Some additional insights into the validity of these assignments can be gleaned from the vibronic structure observed in the absorption spectrum of the 290 nm singlet transition at 14 K. The considerable spectral congestion in this region coupled with the modest resolution of many of the peaks precludes a detailed Franck–Condon analysis; however, a qualitative analysis of the data does suggest that a high-frequency mode corresponding to the terminal V=O stretch is active.

The frequencies of the modes resolved in the spectrum (Figure 9) are tabulated in Table 2. Treating all the data as a single progression yields an average vibrational frequency of 511 cm^{-1}. This value has a large standard deviation (±115 cm^{-1}), and

Table 2. Frequencies (cm^{-1}) of Vibrational Modes Resolved in the 289 nm Singlet Absorption Spectrum of Pseudotetrahedral Oxovanadium Centers in Silica Xerogel

frequency	frequency change	frequency (mode 1)	frequency (mode 2)
35 695			
	344		
35 351		955	
	611		
34 740			1075
	464		
34 276		1045	
	581		
33 695			1083
	502		
33 193		996	
	494		
32 699			1112
	618		
32 081		1000	
	382		
31 699			1097
	715		
30 984		1080	
	365		
30 619			
mean	508 ± 115	1015 ± 48	1092 ± 16

further scrutiny of the data shows that it appears to alternate with some regularity between a frequency of ~400 and ~600 cm^{-1}, suggesting that instead of a single low-frequency mode, two high-frequency modes may be active. Consistent with this suggestion, attempts to duplicate the resolved modes occurring between 30 000 and 36 000 cm^{-1} with a single low-frequency progression were unsuccessful while quite good agreement was attained by employing two progressions at 1015 and 1092 cm^{-1} (Figure 9).

While it might be argued that, within the limits of the experimental error, the 1015 cm^{-1} mode actually corresponds to the 977 cm^{-1} progression seen in the emission, the 1092 cm^{-1} mode clearly cannot and, in fact, can *only* be ascribed to the terminal V=O stretch which has the highest vibrational frequency found in the pseudotetrahedral oxovanadium group. The observation of a vibrational progression associated with the V=O stretch in an electronic transition that is of different symmetry than the emissive state is consistent with our state assignment and with our reassignment of the 977 cm^{-1} progression in the emission.

The assignments obtained for the spectroscopic transitions observed in silica-bound pseudotetrahedral oxovanadium can

be summarized as follows. The $^1A_1$ ground state is of a $(e)^4(a_2)^2$ configuration with the highest occupied molecular orbital being a nonbonding orbital localized on the basal plane oxygens. The first energy excited state is an ^3E arising from the $(e)^4(a_2)^2(e^*) \rightarrow (e)^4(a_2)^1(e^*)^1$ one-electron promotion [$^1A_1 \rightarrow {}^3E$] which can be described qualitatively as a ligand-to-metal charge transfer (LMCT) from the basal plane oxygens. The first well-resolved singlet transition at 290 nm, however, is not to the singlet state associated with the low-energy triplet but is instead to an $^1A_1$ state, resulting from the $(e)^4(a_2)^2(e^*) \rightarrow (e)^3(a_2)^2(e^*)^1$ one-electron orbital promotion [$^1A_1 \rightarrow {}^1A_1$] which can be thought of as a $\pi \rightarrow \pi^*$ V=O transition. The higher energy and more intense singlet band at 240 nm is assigned to an ^1E state also arising from the $(e)^4(a_2)^2(e^*) \rightarrow (e)^3(a_2)^2(e^*)^1$ [$^1A_1 \rightarrow {}^1E$] promotion. The $^1A_1 \rightarrow {}^1E$ transition associated with the emissive triplet state (^3E) is not resolved spectroscopically, and its energy remains unknown. However, as the singlet−triplet splitting is expected to be relatively small ($\approx$1000 cm^{-1}), the absorption for this transition should occur around $\approx$312 nm, heavily overlapping the $^1A_1 \rightarrow {}^1A_1$ band.[25] Finally, on the basis of similar singlet−triplet splitting arguments, we speculate that the ^1E state associated with the $(e)^4(a_2)^2(e^*) \rightarrow (e)^4(a_2)^1(e^*)^1$ [$^1A_1 \rightarrow {}^1E$] transition and the $^3A_1$ state associated with the $(e)^4(a_2)^2(e^*) \rightarrow (e)^3(a_2)^2(e^*)^1$ [$^1A_1 \rightarrow {}^3A_1$] 290 nm singlet transition are in the broad tail of the absorption envelope between 295 and 340 nm. The presence of these overlapping bands in the absorption envelope can be inferred from the long gradual increase in the polarization anisotropy in this region.

There are a number of significant conclusions that can be drawn about the unique reactivity of the pseudotetrahedral oxovanadium group and its relationship to the electronic structure described here. First, the lowest energy excited state involves promotion of an electron from the basal plane ligands to the metal center and not from the terminal V=O bond.

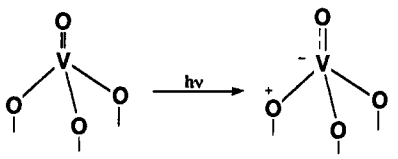

This differs substantially from the numerous descriptions of this excited state presented previously. The misassignment of this state in the past is due in part to a lack of detailed spectroscopic data (particularly absorption spectra) which we have been able to obtain due to the transparency of these xerogel materials. Contributing to this, however, has been the *a priori* assumption that because the photochemistry of these species ultimately involves the terminal V=O bond, a local excitation of that chromophore must necessarily be involved in the formation of the excited state. This assumption is specious as the excited state assigned here, based on spectroscopic arguments, is entirely consistent with the observed photochemistry. The e* orbital to which the electron is promoted in the excited state is antibonding with respect to the terminal V=O ligand and will reduce its formal bond order, thereby "activating" it. Also implicit in this excited state description is that other factors not previously considered may be important. For example, the fact that electron density is removed from the basal plane ligands may affect the orientation of substrates in bimolecular reactions with the excited state. It is also well known that the excited triplet state of these species has a high degree of radical character. This can be inferred from their facility in initiating polymerizations and in performing atom abstraction processes. Historically, on the basis of misconceptions as to the nature of the excited state, these processes have been viewed as taking place via the unpaired electron on the terminal oxygen. In light of the electronic structure presented here, it is clear that while the terminal V=O bond may ultimately be affected, the origin of the photochemical process is likely to be at the metal center.

Our understanding of the ground state structure of these species, with the HOMO centered on the basal plane oxygens, has a number of implications for thermal reactivity as well. Deo et al. noted that the frequency of the terminal V=O stretch remained relatively constant regardless of substrate, suggesting that the bridging oxygens must be responsible for substrate effects.[26] The possibility that the basal plane ligands can exert a strong effect on the metal center has been discussed in detail by Feher et al. in relation to the structure of relevant oxovanadium model compounds.[27] These observations are quite consistent with the description of the electronic structure presented here. Different substrates, through electronic interactions, will directly affect the energy of the a_2 HOMO, in effect modulating its relative energy and thereby affecting the reactivity. For example, going from a silicate to a titanate substrate should result in a lowering of the energy of the a_2 nonbonding orbital due to the electron withdrawing (*i.e.*, "π" type interactions) of the vacant d orbitals on the Ti^{4+}. These electronic effects would be in addition to any changes in coordination geometry induced in the oxovanadium group when bound to different substrates—notably, such coordination changes may also affect the energy of the a_2 orbital. In addition to the electronic interaction, the ground state will be vibronically coupled to the substrate, which, in high-temperature catalytic processes, may be important as a mechanism for activating the terminal V=O bond. For example, at high temperatures the low-frequency vibronic modes which couple the substrate to the basal plane ligands, and hence directly to the ground state HOMO, will be populated, thereby mixing the ground state with other low-energy states of the oxovanadium center. In general, we believe that the description of the electronic structure of silica-bound oxovanadium afforded by this investigation will have a significant impact on understanding the reactivity of these species in important catalytic systems.

Acknowledgment. A.E.S. would like to thank Dr. Jay Winkler of the Beckman Institute at Caltech and Prof. Jeff Zink of the University of California, Los Angeles for helpful discussions and Heidi Youngkin for invaluable assistance in the preparation of this manuscript. A portion of this work was carried out at the Jet Propulsion Laboratory, California Institute of Technology under a grant from the Directors Discretionary Fund. Support was also provided by the Committee on Research at the University of California, Riverside.

JA942834L

(25) Charge transfer transition will generally have small singlet−triplet splitting as the distance between the two unpaired electrons greatly reduces spin−spin interactions. The singlet−triplet splittings of vanadate (VO_4^{3-}) are 200 and 1000 cm^{-1} for the $^1A_1 \rightarrow {}^3T_1$ and $^1A_1 \rightarrow {}^3T_2$ transitions, respectively ($t_1 \rightarrow e$ transitions) (ref 7d and Van Tol, J.; Van Hulst, J. A.; Van Der Waals, J. H. *Mol. Phys.* **1992**, *76*, 547). Transitions associated with the V=O group on the oxovanadium should readily fall into this range as it has a similar orbital heritage. LMCT bands from the basal plane ligands will, if anything, have smaller splittings due to the longer V−O bond length and the diminished "π" bonding and, hence, the electron correlations associated with it.

(26) Deo, G.; Eckert, H.; Wachs, I. E. *Abstracts of Papers*, 199th National Meeting of the American Chemical Society, Boston, MA, Spring 1990; American Chemical Society: Washington, DC; p 16.

(27) Feher, F. J.; Walzer, J. F. *Inorg. Chem.* **1991**, *30*, 1689.